

Quantitative determination of polymorphic composition in intact compacts by parallel-beam X-ray powder diffractometry

Wenjin Cao^a, Simon Bates^b, Garnet E. Peck^a, Peter L.D. Wildfong^a,
Zihui Qiu^a, Kenneth R. Morris^{a,*}

^a Department of Industrial and Physical Pharmacy, School of Pharmacy, 1336 Robert E. Heine Pharmacy Building, Purdue University, West Lafayette, IN 47907-1336, USA

^b Kratos Analytical, Inc., 100 Red Schoolhouse Road, Building A, Chestnut Ridge, NY 10977-7049, USA

Received 25 October 2001; received in revised form 26 June 2002; accepted 7 July 2002

Abstract

This paper details the development of a method using parallel-beam X-ray powder diffractometry as a novel means of determining polymorphic composition in intact compacts. Two polymorphic systems, chlorpropamide and glycine, were selected. The polymorphic components were weighed, mixed, and compressed using a Carver press with 3/8-in. concave tooling. The compacts were then analyzed using parallel-beam X-ray powder diffractometry in transmission geometry. The data were processed using the profile-fitting module in the Shimadzu XRD-6000 software V 4.1 (for NT 4.0/98). The integrated intensity ratio of a selected peak for each crystal form was used for quantitation of each polymorph. Excellent linear correlation was observed for both polymorphic systems. The convex shape of the compact surface had no effect on the XRD patterns. Since parallel-beam X-ray diffractometry is not sensitive to the shape of the sample surface, it provides a simple method for quantifying polymorphs in intact compacts. Further work to extend this to formulated tablets is ongoing. The relatively larger variation in one of the peaks in the chlorpropamide study was found to be consistent with the computational analysis of the slip behavior of the stable polymorph. This method provides the first reported non-invasive X-ray diffraction pattern quantitation of crystal forms in intact compacts.

© 2002 Elsevier Science B.V. All rights reserved.

Keywords: Parallel-beam X-ray powder diffraction; Chlorpropamide; Glycine; Polymorph; Quantitation; Compact; Process-induced transformation

1. Introduction

X-Ray powder diffraction (XRPD) is the primary tool for the study of most polymorphic

transformations. Process-induced transformations have been observed and documented by many investigators [1–4]. Traditional methods to detect phase changes in compressed tablets require either grinding or sectioning suspect tablets, which may introduce unwanted artifact, further transformations, and add significant time to the method development and execution. The work reported

* Corresponding author. Tel.: +1-765-496-3387; fax: +1-765-494-6545

E-mail address: morriskr@purdue.edu (K.R. Morris).

here summarizes efforts to develop a method to detect phase changes in an intact compact.

Typical powder X-ray diffraction instruments have primarily used Bragg–Brentano para-focusing geometry. It is an excellent configuration for providing high resolution without sacrificing peak intensity. However, Bragg–Brentano imposes certain geometric restrictions on specimens and small deviations may significantly influence the instrumental resolution and precision. In the para-focusing geometry, there are three systematic errors associated with the specimen properties: flat specimen error, transparency error, and specimen displacement error [5].

Flat specimen error occurs because the surface of a packed powder specimen is typically flat and does not conform to the curvature of the focusing circle [5]. This also affects peak shape and causes asymmetric peak broadening.

Errors from specimen transparency are introduced when the samples have small linear attenuation coefficients (e.g. organic pharmaceutical compounds) and the X-ray beam penetrates many cells below the surface of the analyzed specimen. Consequently, the average diffracting surface lies below the physical surface of the specimen. X-ray beam penetration causes the effective specimen surface to lie below (or above) the focusing circles. This effect is known as specimen displacement. Both errors make the study of intact tablets difficult or impossible.

Most of these errors can be minimized in a non-focusing parallel-beam geometry. With collimated X-ray radiation and a crystal analyzer or “angular slit”, the displacement-related aberrations are greatly reduced or eliminated. All diffracted rays that satisfy the Bragg conditions are recorded at the analyzer simultaneously, independent of their point of origin in the sample [6], as illustrated in Fig. 1. This means that the diffracted X-rays are no longer bound by a diffraction geometry since there are no focusing circles in parallel-beam geometry. The X-rays diffracted by the sample are parallel and recorded at the crystal analyzer at the same time. Thus the diffraction peaks will show up at the correct 2θ angles (i.e. those that satisfy the Bragg conditions).

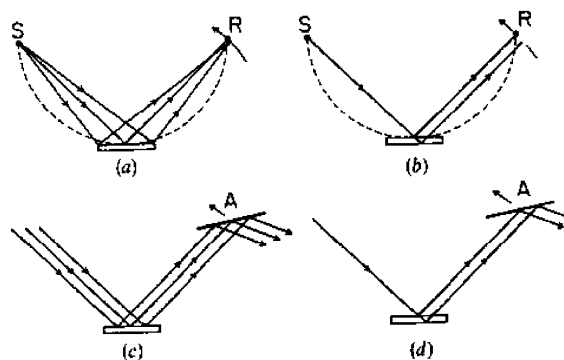


Fig. 1. Scattering geometry for powder diffraction illustrating effect of (a) flat specimen, (b) specimen transparency in a conventional focusing geometry and the corresponding effects with parallel-beam geometry (c) and (d). S, R, and A denote source, receiving slit, and analyzing crystal, respectively (from [6]).

A powder diffractometer with the incident beam collimator and slits replaced by a parallel-beam poly-capillary optic (designed by X-ray Optical Systems, Inc.) was employed for our studies. The poly-capillary optic allows the collection of X-rays from a standard line source in point focus orientation and collimates them into a quasi-parallel beam with FWHM (full width half maximum) divergence of 0.25° at Cu $K\alpha$ wavelengths. The optic as installed, operates in true parallel-beam geometry, thus eliminating the focusing errors associated with Bragg–Brentano geometry. The relaxation of the sample height restriction also allows the study of irregularly shaped samples.

In XRPD quantitation studies, preferred orientation effects can sometimes be very significant, a phenomenon often exacerbated by compaction owing to the tendency of crystallites orient during the process. In this study, transmission geometry was used to minimize some of the possible preferred orientation effects. In transmission mode, compacts were oriented perpendicular to the incident X-ray beam (Fig. 2). As a result, diffraction occurs from planes normal to the compact surface. In ordinary reflection geometry, the effects of preferred orientation may be amplified because the depth of penetration varies with the angle of incidence and does not fully represent the arrangement of the crystal throughout the measured depths. In transmission mode, however,

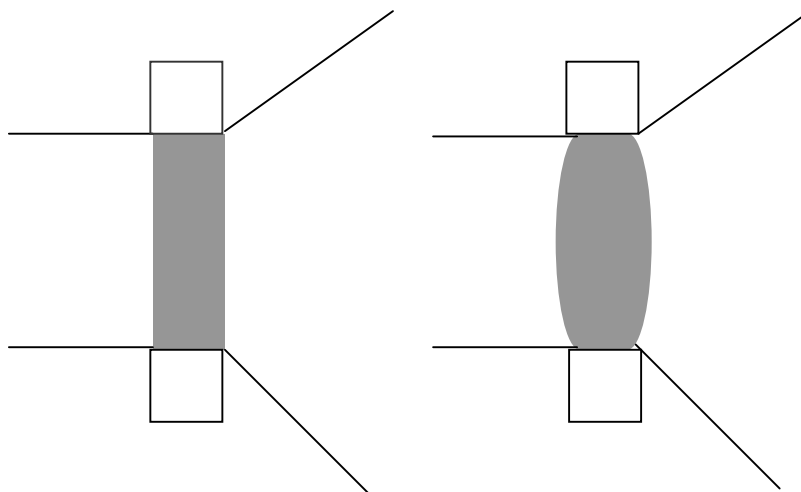


Fig. 2. A schematic diagram shows the whole compacts (flat-faced or convex) was analyzed by XRPD in the transmission mode.

the depth of X-ray beam penetration is constant and irradiates the entire compact (as configured), providing a more complete average of sample orientations than in the reflection mode. This does not eliminate preferred orientation but the impact should be faithfully preserved as a function of d -spacing and, therefore, be more readily identified and modeled.

One of the characteristics of parallel-beam geometry is that the generated X-ray peak profile shape is very nearly Gaussian. Furthermore, the shape does not vary with the scanning angle allowing the use of one simple function to describe the entire profile. This is especially useful in profile-fitting analysis, which uses mathematical functions to model the X-ray profile and separate each peak. Once the peaks have been separated (deconvoluted) and expressed by a function (e.g. Gaussian), an accurate integrated intensity can be calculated. So the fact that the X-ray profiles can be described by a single Gaussian function for the whole scanning range makes profile fitting much easier and typically more accurate for the parallel-beam geometry than for the Bragg–Brentano geometry.

Of course complicating any such analysis is the fact that crystals fracture, deform, orient, and may undergo crystal form transformations during compaction. An understanding of the cleavage/slip properties of the crystals in this study was pursued

to allow more complete interpretation of the XRPD patterns for compressed compacts.

2. Experimental

2.1. Materials

Chlorpropamide Form A (Lot 31H0722) was obtained from the Aldrich Chemical Company of St. Louis, MI, and used as-received. Form C was prepared by heating crystals of Form A at 115 °C for 3 h, followed by gently grinding before use.

Both glycine crystal forms were obtained by recrystallizing the commercially available compound from water (Mallinckrodt, Phillipsburg, NJ). A glycine/water solution with a concentration of twice the saturation concentration was prepared at 25 °C. The solution was heated until all glycine dissolved at 75 °C and then the resulting solution was cooled to room temperature. Rapid cooling with agitation yielded the α -form, whereas slow cooling without agitation produced the γ -form. The γ -form was left in the mother liquor for 1 week prior to analysis [7]. Both forms were ground manually in a mortar and pestle, and then passed through a US-mesh No. 230 sieve (63 μ m).

2.2. Preparation of glycine compacts

Mixtures containing known varying weight fractions of glycine α - and γ -forms were prepared. Each mixture had a total weight of approximately 0.1500 g. The concentration of mixtures was varied from 0 to 100% in 10% increments of the α -form. Each mixture was weighed individually and compressed. To our knowledge, no polymorphic transformation of glycine under compression has been reported; therefore, a pressure of 36 200 psi with a 20 s dwell time was used in preparing the compacts. In addition, the XRPD patterns of the pure glycine forms compressed at the experimental pressure did not show transformation at detectable levels. To test the ability of analyzing irregularly shaped samples with the parallel-beam X-ray setup, compacts were made using 3/8-in. concave tooling, which produced compacts having a central band thickness of approximately 2.5 mm. The compacts were then placed in aluminum X-ray sample holders having a central cavity commensurate with the size of the compacts, allowing them to be held in by friction for X-ray analysis.

2.3. Preparation of chlorpropamide compacts

Pure chlorpropamide (CPM) compacts were prepared and analyzed in the same manner as above. Each CPM compact weighed approximately 0.1200 g. Since chlorpropamide was reported to undergo polymorphic transformation and/or amorphous formation during compression [2–4], compacts were compressed at a pressure of 905 psi using a Carver press (Model C, Fred S. Carver, Inc., WI) with a 10 s dwell time. The compression pressure was chosen because it is below the transition pressures of chlorpropamide either reported in the literature [2] or observed in our laboratory. It is also the lowest pressure that chlorpropamide polymorphs can easily form compacts under compression.

2.4. X-ray powder diffraction

XRPD measurements were made on a Shimadzu XRD-6000 X-ray diffractometer (Kratos Analytical, Inc., NY) fitted with an XOS[®] poly-capillary

X-ray optic (X-ray Optical Systems, Inc., NY) on the incident beam side, which produced a 10×10 mm² square spot. This poly-capillary optic, together with a secondary collimator and monochromator, allows the generation of an X-ray beam with extremely high intensity. Compacts were measured in transmission mode with θ fixed at 90° while 2θ was scanned over the desired range at a speed/step of $4^\circ/\text{min}/0.04^\circ$. The scanning range was $10\text{--}35^\circ$ and $10\text{--}50^\circ$ for chlorpropamide and glycine, respectively. Shimadzu profile-fitting analysis was used to generate integrated intensity of the selected peaks (Shimadzu XRD-6000 software version 4.1).

2.5. Differential scanning calorimetry

Chlorpropamide compacts were checked for possible formation of amorphous material following compression. Differential scanning calorimetry (DSC) measurements were made using a TA 2920 differential scanning calorimeter (TA Instruments, DE). The experiments were conducted using a $10^\circ\text{C}/\text{min}$ heating rate. Chlorpropamide compacts produced for quantitative analysis were also studied using DSC to check for possible inter-conversions of crystal forms induced during compaction. These compacts were compressed using the same pressure indicated for quantitative analysis, and lightly deagglomerated into powders for immediate analysis using a mortar and pestle. Approximately 2–4 mg representative samples were used for each analysis.

2.6. Attachment energy calculation

Attachment energy calculations were carried out using Cerius² software (Molecular Simulations, Inc., San Diego, CA). The calculation method was based on the work by Osborn et al. [8]. Attachment energies were calculated for chlorpropamide Form A from the crystal structure obtained from the Cambridge Structural Database (Cambridge Crystallographic Data Center, Cambridge, UK).

DREIDING 2.21 was the force field in the study, and structural optimizations of the crystal

were predicted by the minimization of the total lattice energy.

3. Results and discussion

3.1. Calibration curves for glycine compacts

The experimental powder X-ray diffraction patterns of glycine α - and γ -forms were identical to the calculated powder patterns with respect to d -spacing. The XRPD peaks at $2\theta = 19^\circ$ for the α -form and 21° for the γ -form were selected for quantitative analysis (Fig. 3).

The XRPD peak intensity ratio of the γ -form reflection to the α -form vs. the corresponding concentration ratio in the range 0–100% γ -form in α -form is a linear function ($y = 1.47x - 0.00335$ with a correlation coefficient equal to 1.00; Fig. 4). Since each sample for each compact was weighed individually, and the entire compact was analyzed by X-ray, only one sample was necessary at each concentration. The statistic was rather improved by sampling at more frequent regularly spaced concentrations.

Both sides of each compact were measured facing the incident X-ray beam to address the possibility that non-uniformity of the polymorphs in the compacts or variable absorption characteristics would affect their X-ray peak intensities. No significant peak intensity difference was found for

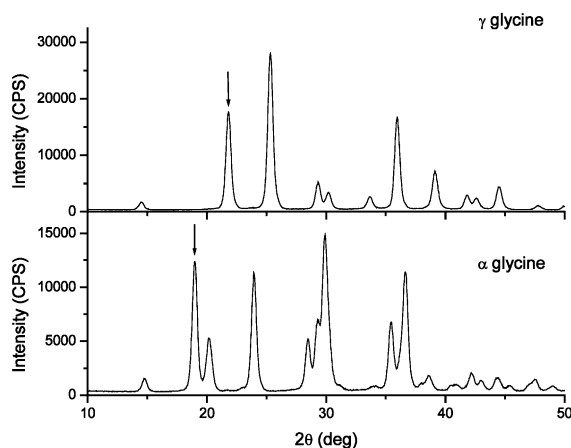


Fig. 3. The XRPD pattern of glycine α -form and γ -form.

the different sides of each compact, indicating that data collected on one side were sufficient.

3.2. Calibration curves for chlorpropamide compacts

The phase purity of Form A was confirmed by the comparison of the experimental powder X-ray diffraction patterns to the calculated pattern. The single-crystal structure of Form C has not been reported; thus, we established the purity of Form C by monitoring the disappearance of the form A peaks during solid transformation from Form A to Form C. The XRPD peaks at $2\theta = 11.7^\circ$ for Form A and 15.0° for Form C were chosen for quantitative analysis based on the resolution and lack of mutual interference (Fig. 5).

As mentioned, chlorpropamide undergoes polymorphic inter-conversion during compression [2–4]. During method development, therefore, special care was taken to apply the lowest possible compression force that resulted in suitable compacts during preparation. These compacts were analyzed immediately after compression using DSC and XRPD. From DSC analysis, neither phase transformed between the two forms, nor was the formation of an amorphous phase observed in the compacts (Fig. 6).

The XRPD peak intensity ratio of Form C to Form A vs. the corresponding concentration ratio has a linear relationship ($y = 0.29x - 0.0067$ in the concentration range 0–100% with a correlation coefficient 0.99; Fig. 7). It was observed that if the peak intensity was used for quantitation instead of the peak intensity ratio, the peak picked for Form C gave a much better correlation with the concentration than the peak of Form A. This suggests that the chosen peak for Form A has a larger variation in peak intensity compared to that of Form C ($y = -2.5 \times 10^3x + 2.5 \times 10^3$; $R^2 = 0.99$ for Form C, and $y = 7.5 \times 10^3x + 2.5 \times 10^2$; $R^2 = 0.96$ for Form A; see Fig. 8).

3.3. Attachment energy calculation of chlorpropamide

In a recent publication, Sun and Grant [9] showed that compression can induce cleavage in

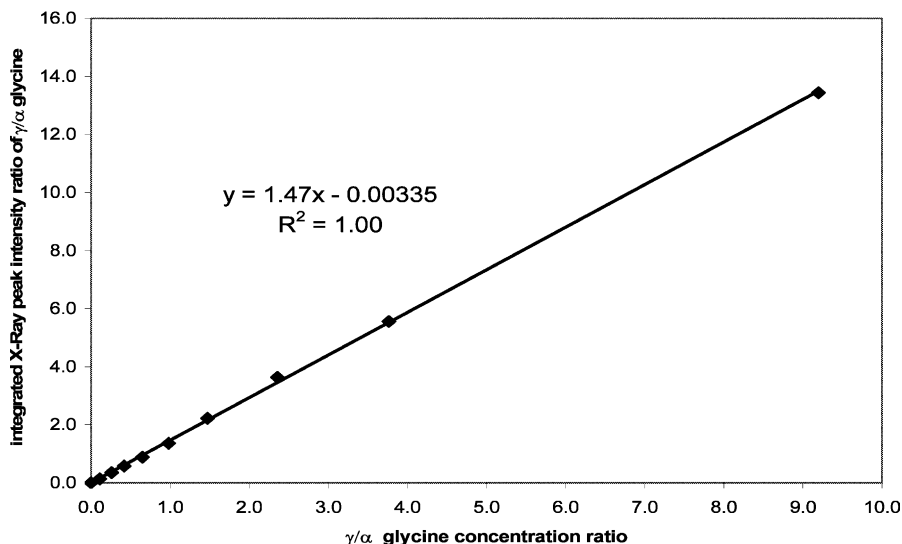


Fig. 4. Plot of XRPD-integrated peak intensity ratio of glycine α -form/ γ -form vs. the corresponding concentration ratio.

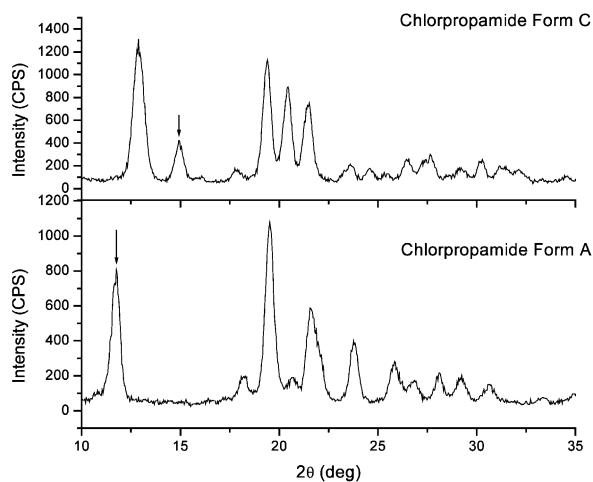


Fig. 5. The XRPD pattern of chlorpropamide (CPM) Forms A and C.

crystalline materials, thus increasing the exposure of those surfaces that lie parallel to the cleaved direction. Planes exhibiting large variations in peak intensity are often slip planes. This is due to the fact that slip planes tend to be more widely spaced (larger d -spacing) and, typically, exhibit lower attachment energy. Compression may result in the activation of a slip system generating new faces that may be preferentially oriented relative to

the direction of the applied force. Compression may increase the exposure of those surfaces that lie parallel to slip planes within the crystal. Upon cleaving, the newly exposed surfaces may have a higher probability of lying parallel to the diffraction plane. As a result, the diffraction peaks corresponding to families of slip planes may exhibit higher XRPD intensities following compaction. This may contribute the intensity variations reported here.

Computation of attachment energies of key slices of chlorpropamide polymorph Form A was carried out to predict the potential slip planes. According to Osborn's method [7], slip planes are predicted based on the attachment energy associated with the growth of a crystal face with Miller indices $(h k l)$. The slices exhibiting the lowest attachment energy have the highest probability of being a slip plane. From calculations during growth morphology prediction, it was found that the $(1 0 2)$ -plane had among the lowest attachment energies, suggesting that it may have a high proclivity for slip. This result implies that the variation of X-ray peak intensity might be due to the crystal cleavage under compression, allowing preferential exposure of certain planes. Table 1 shows the three planes with the lowest calculated

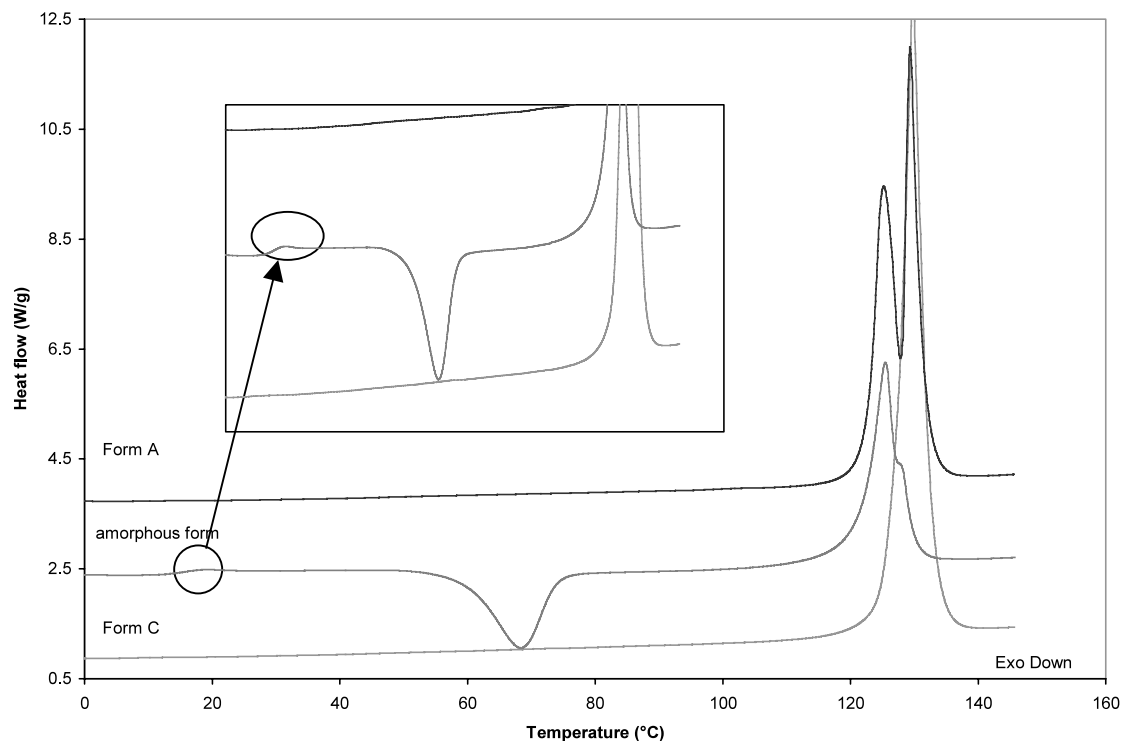


Fig. 6. The DSC thermogram of chlorpropamide. The top thermogram is for pure Form A after compression, which melts, transforms, and melts again at 125 and 129 °C, respectively. The middle thermogram shows the amorphous chlorpropamide, which has a glass transition temperature of 16 °C, recrystallizes at 68 °C, and melted at 125 °C. The bottom thermogram is for pure Form C after compression, which melts at 129 °C.

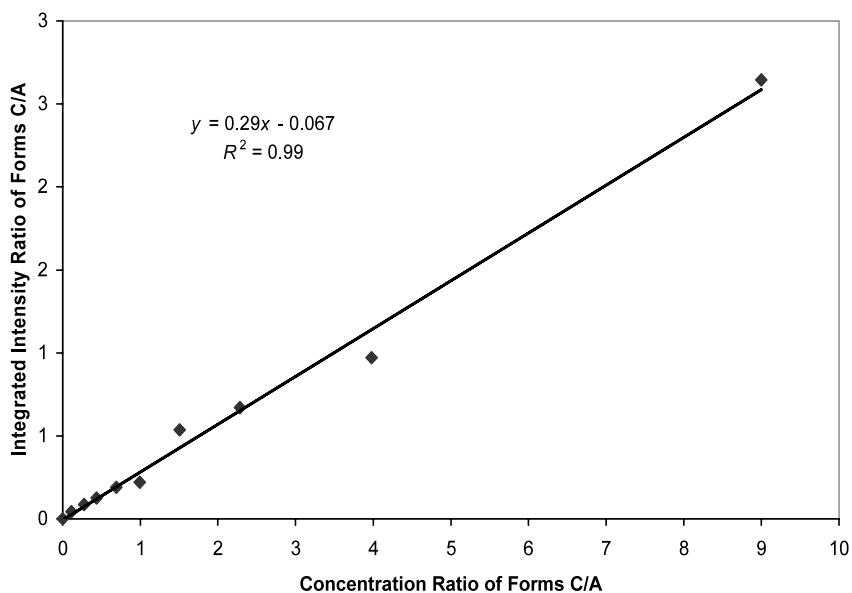


Fig. 7. Plot of XRPD-integrated peak intensity ratio of chlorpropamide Forms C/A vs. the corresponding concentration ratio.

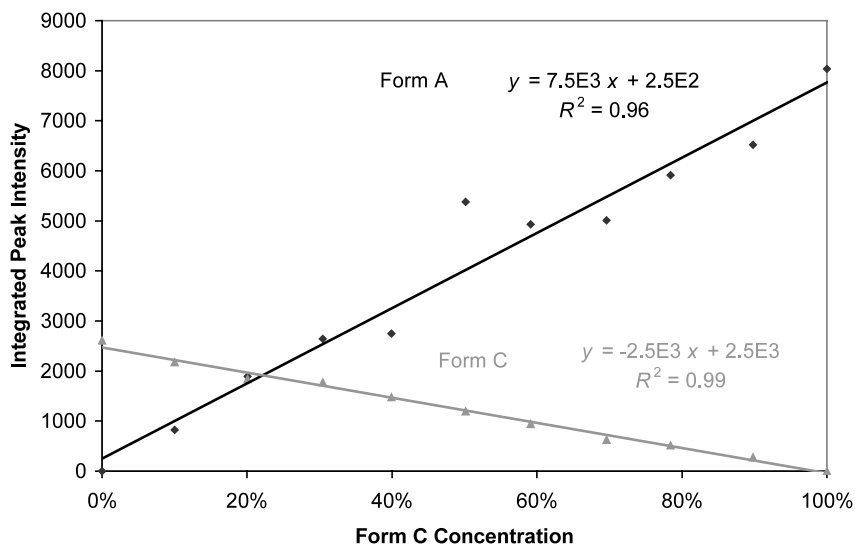


Fig. 8. The integrated peak intensities of Forms A and C vs. the corresponding concentrations of polymorph mixtures.

Table 1
Attachment and lattice energies of chlorpropamide Form A

| Plane (<i>h k l</i>) | Energy (kcal/mol) |
|------------------------|-------------------|
| 0 0 2 | −53 |
| 1 0 1 | −65 |
| 1 0 2* | −80 |
| Lattice energy | −237 |

attachment energy (the suspected slip plane is marked with an asterisk).

4. Conclusion

A method was developed to analyze quantitatively the polymorphic content in intact compacts using parallel-beam XRPD. Parallel-beam XRPD is insensitive to the surface profile of the samples making intact analysis possible. Analysis in transmission as opposed to reflectance helped to minimize the preferred orientation effects in the samples. Moreover, profile-fitting data analysis separates overlapping peaks and allows accurate peak areas to be determined. This method works

much better with parallel-beam geometry since the peak shapes obtained are symmetrical and invariant with respect to the scanning angles. Analysis of the slip system in crystals can qualitatively explain the relatively larger variation in one of the peaks in the chlorpropamide study, and may ultimately be used to refine the method. This work represents the first report we are aware of quantifying polymorphic form ratios in intact compact/tablets.

A study to apply the developed method to analyze the formulated tablets is currently being carried on in our laboratory. The biggest challenge in analyzing tablets comes from the excipient based interferences. The addition of excipients affects the method in two ways: (1) the XRPD peak interferences from the excipients may make it difficult to pick a well-resolved peak for quantitation; (2) the “dilution effect” of excipients on the XRPD peak intensity may not be easily predicted. As mentioned in Section 1 that one advantage of the parallel-beam XRPD is that it generates symmetrical Gaussian peaks, which makes it easier to separate the overlapping peaks using the mathematical tools. The authors have developed a quantitative model to address the XRPD intensity variations as a function of sample thickness

and solid fractions. This is a subject of a second publication in preparation for submission within a month of this writing. With this model, the “dilution effect” is accounted for and the peak intensities can be normalized.

Acknowledgements

The authors would like to thank the National Science Foundation Industry, University Process Research Center at Purdue University, for funding and XOS for their technical support and J.C. Osborn for his advice.

References

- [1] H.K. Chan, E. Doelker, *Drug Dev. Ind. Pharm.* 11 (1985) 315–332.
- [2] M. Otsuka, T. Matsumoto, N. Kaneniwa, *J. Pharm. Pharmacol.* 41 (1989) 665–669.
- [3] M. Otsuka, Y. Matsuda, *Drug Dev. Ind. Pharm.* 19 (1993) 2241–2269.
- [4] T. Matsumoto, N. Kaneniwa, S. Higuchi, M. Otsuka, *J. Pharm. Pharmacol.* 43 (1991) 74–78.
- [5] R. Jenkins, R.L. Snyder, *Introduction to X-ray Powder Diffractometry*, Wiley, New York, 1995, pp. 200–209.
- [6] J.B. Hastings, W. Thomlinson, D.E. Cox, *J. Appl. Cryst.* 17 (1984) 85–95.
- [7] T. Davis, Personal communication.
- [8] J.C. Osborn, P. York, R.C. Row, R.J. Roberts, *Int. Symp. Ind. Cryst.* 14 (1999) 1166–1174.
- [9] C. Sun, D.J.W. Grant, *J. Pharm. Sci.* 90 (2001) 569–579.